View metadata, citation and similar papers at core.ac.uk

brought to you by CORE

provided by Radboud Repository

Radboud Repository

Radboud University Nijmegen

PDF hosted at the Radboud Repository of the Radboud University Nijmegen

The following full text is a publisher's version.

For additional information about this publication click this link.
http://hdl.handle.net/2066/149444

Please be advised that this information was generated on 2017-12-05 and may be subject to change.

PCCP

PAPER

View Article Online
View Journal | View Issue

Published on 05 October 2015. Downloaded by Radboud Universiteit Nijmegen on 01/02/2016 10:52:33.

Cite this: *Phys. Chem. Chem. Phys.*, 2015, **17**, 29064

Formation of polycyclic aromatic hydrocarbons from bimolecular reactions of phenyl radicals at high temperatures†

P. Constantinidis,[a] H.-C. Schmitt,[a] I. Fischer,[a] B. Yan[b] and A. M. Rijs[b]

Received 8th September 2015,
Accepted 5th October 2015

DOI: 10.1039/c5cp05354d

www.rsc.org/pccp

The self-reaction of the phenyl radical is one of the key reactions in combustion chemistry. Here we study this reaction in a high-temperature flow reactor by IR/UV ion dip spectroscopy, using free electron laser radiation as mid-infrared source. We identified several major reaction products based on their infrared spectra, among them indene, 1,2-dihydronaphthalene, naphthalene, biphenyl and *para*-terphenyl. Due to the structural sensitivity of the method, the reaction products were identified isomer-selectively. The work shows that the formation of indene and naphthalene, which was previously considered to be evidence for the HACA (hydrogen abstraction C_2H_2 addition) mechanism in the formation of polycyclic aromatic hydrocarbons and soot can also be understood in a phenyl addition model.

Introduction

It is one of the main goals in combustion chemistry to understand the formation of polycyclic aromatic hydrocarbons (PAH) and soot, because of the carcinogenicity and the negative environmental impact of the compounds.[1,2] A key step is the formation of the first ring, *i.e.* phenyl radical or benzene, which is assumed to be the result of bimolecular reactions of C_3 units,[3–5] or possibly a reaction between C_4 and C_2 hydrocarbons.[6] Several models were developed for the subsequent growth to larger units.[7] One major pathway for PAH formation is assumed to be the HACA mechanism (hydrogen abstraction C_2H_2 addition).[8,9] As it was pointed out that HACA might be too slow to explain the formation of large PAH,[1,10] the condensation of aromatic rings, in particular phenyl, was suggested to be an alternative pathway, explored for example by Comandini *et al.*[11] and by Shukla and Koshi.[12] The mechanistic questions are not settled due to the lack of direct experimental data. Due to the large number of reactive intermediates that appear in a real flame, it is very difficult to draw conclusions on the reaction pathways. Therefore, it is important to conduct controlled studies with only a few reactants to get insight into combustion chemistry. Reactions starting from phenyl are particularly relevant. However, the seemingly simple phenyl condensation has not been investigated extensively yet. A laser photolysis/mass spectrometry study yielded rate constants and temperature-dependent Arrhenius parameters for the dimerisation.[13] In a recent shock tube study employing iodobenzene as a precursor Tranter *et al.* found that the direct dimerization of phenyl is accompanied by a disproportionation to benzene + benzyne with a comparable rate (I).[14]

$$2\ C_6H_5 \rightarrow C_6H_6 + C_6H_4 \qquad \text{(I)}$$

This formation of further species in the first bimolecular reaction thus opens additional reaction channels. Product information in previous work on phenyl reactivity was often extracted from mass spectra (MS) of reaction products obtained by electron impact ionisation,[14] by 118 nm photoionisation[12] or by GC/MS.[11] However, only limited information on the molecular structure is available from these techniques, in particular when several product isomers can be formed. Given the complexity of the phenyl system, it is therefore essential to investigate its products by a structure-sensitive method.

It is been shown that high temperature flow (pyrolysis) microreactors[15] provide a suitable environment to investigate combustion processes[16] and can be combined with the tools of gas-phase spectroscopy, which gives the opportunity to test theoretical predictions. The flow dynamics in such a reactor has been analysed in detail.[16] Ellison and coworkers studied the thermal decomposition of compounds like furan[17] and anisole.[18] Recently, the work was extended to the decomposition of the benzyl radical.[19] Under suitable conditions a pyrolysis reactor also provides access to bimolecular condensation reactions. In such experiments, PAH molecules have been detected by photoionization mass spectrometry with tunable synchrotron radiation (SR), which provides structural information through the ionization energy (IE). Bimolecular reactions in the pyrolysis

[a] *Institute of Physical and Theoretical Chemistry, University of Würzburg, Am Hubland, D-97074 Würzburg, Germany. E-mail: ingo.fischer@uni-wuerzburg.de*
[b] *Radboud University, Institute for Molecules and Materials, FELIX Laboratory, Toernooiveld 7-c, 6525 ED Nijmegen, The Netherlands. E-mail: a.rijs@science.ru.nl*

† Electronic supplementary information (ESI) available. See DOI: 10.1039/c5cp05354d

This journal is © the Owner Societies 2015

Published on 05 October 2015. Downloaded by Radboud Universiteit Nijmegen on 01/02/2016 10:52:33.

reactor were already observed in early work combining pyrolysis with SR.[20] Parker *et al.* studied a mixture of phenyl and acetylene to confirm the validity of the HACA mechanism.[21] In the reaction of phenyl and C_3H_4 they identified for example indene and naphthalene as reaction products.[22] On the other hand, more recent results on a naphthyl/acetylene mixture cast doubts on the relevance of the HACA mechanism.[23] The large number of possible isomers that cannot easily be distinguished by their ionization energy limits the usefulness of photoionization mass spectrometry for larger molecules. More detailed information on reaction products is obtained, when ions and photoelectrons are detected in coincidence.[24–26] We recently showed that IR/UV ion dip spectroscopy is a powerful, alternative tool to study high temperature reactions in a flow reactor, since it combines the structural sensitivity of infrared spectroscopy with mass information.[27,28] In this technique, molecules are ionised by [1+1] resonance-enhanced multiphoton ionisation (REMPI) with UV laser radiation. The ground-state IR spectra are obtained by monitoring the depletion in the ionization signal that occurs upon excitation of a vibrational transition, resulting in mass-selected IR spectra. The flux necessary to excite molecules in a free jet in the mid-IR fingerprint region is provided by a free electron laser (FEL). In previous experiments, it was found that the self-reaction of phenylpropargyl radicals leads selectively to *para*-terphenyl and 1-(phenylethynyl)naphthalene.[28] To further understand the combustion relevant reactions leading to PAHs, we will here examine the dimerization of phenyl radical, C_6H_5 itself. Phenyl is among the first aromatic species formed in combustion and thus constitutes the starting point in the growth to larger units. It is the goal of this work to identify isomer-selectively the products formed from phenyl radicals without a further reactant being added.

Experimental

The experiments were carried out at the FELIX free electron laser laboratory at the Radboud University (the Netherlands). The characteristics of the FEL have already been described in the literature.[29,30] It provides a high flux in the fingerprint region that permits to record IR spectra of diluted gaseous samples. The measurements were performed in a differentially pumped molecular beam apparatus.[31] Initial experiments aimed at optimizing the reaction conditions were carried out in the Würzburg laboratory by photoionization mass spectrometry using 118 nm radiation.

All species were produced by flash pyrolysis in a 30–40 mm long SiC tube with an inner diameter of 1 mm, mounted onto a pulsed solenoid valve.[15] In all experiments described below azobenzene, commercially obtained from Aldrich (supposed purity >99%), was employed. It was heated to 130–160 °C to achieve a sufficient vapour pressure and seeded in 1.4 bar of argon. It thermally dissociates according to

$$C_6H_5\text{–}N{=}N\text{–}C_6H_5 \rightarrow 2\ C_6H_5 + N_2 \qquad \text{(II)}$$

The pyrolysis conditions were chosen to promote bimolecular reactions. The skimmed pulsed (10 Hz) free jet enters the ionization region of a time-of-flight mass spectrometer and is crossed by IR and UV laser radiation. A frequency-doubled dye laser, pumped by a Nd:YAG laser was employed for UV excitation. Experiments were carried out at wavelengths of 285 nm, 270 nm, and 255 nm, UV energies were around 1–1.5 mJ. Molecules were ionized in a [1+1] process. The IR-FEL, operating at 5 Hz, was fired typically around 200 ns before the UV laser and scanned over the fingerprint region of the molecule (590–1750 cm^{-1}) with a step width of 2–2.5 cm^{-1}. When the IR light is resonant with a vibrational mode of the species, the ion signal is depleted, because only the molecules left in the ground state can be resonantly ionized. At each wavenumber step we recorded 50 shots with the IR-radiation present and 50 shots without. The signal obtained with the IR-radiation present is then divided by the signal obtained without IR radiation and the decadic logarithm is taken and IR power corrected. The spectra shown below are typically composed of two segments (590–1000 cm^{-1} and 1000–1750 cm^{-1}) that were recorded at a single UV wavelength and averaged over several scans. The spectra were smoothed using the Savitzky–Golay algorithm.

The spectra were assigned to a given isomer with the aid of calculations. Density functional theory (DFT) as implemented in the Gaussian suite of programs was employed.[32] For all molecules the B3LYP functional was used in combination with the 6-311++G(d,p) basis set. All computed harmonic IR frequencies were scaled with an empirical factor of 0.975. To facilitate comparison with the experiment, the calculated spectra were convoluted with a Lorentzian function with a full width at half maximum (FWHM) of 10 cm^{-1}.

Results

Mass spectra

In Fig. 1 the photoionisation mass spectra (PIMS) of the pyrolysis products of azobenzene are depicted. The upper trace shows a spectrum obtained at 118 nm, which is sufficient to ionize almost all molecules in the beam in a one-photon step. Although ionization cross sections are different for different molecules the spectrum gives a reasonably realistic distribution of molecular concentrations in the jet. Note that the precursor azobenzene (m/z = 182) has been completely converted. Dimerization is evident from the peak at m/z = 154. A major parameter to be optimized in the experiment is the delay between gas pulse and laser: early in the gas pulse the amount of bimolecular reactions is small and isolated radicals can be observed, while in the centre of the gas pulse bimolecular reactions become important. Clearly in the 118 nm mass spectrum (Fig. 1, upper trace), benzene (C_6H_6) is one of the largest peaks. Its observation confirms the conclusion of Tranter *et al.* that disproportionation to benzene and benzyne competes with dimerization. Only a small benzyne peak (m/z = 76) is visible in the MS, likely due to its high reactivity. The lower trace depicts the two-photon [1+1] REMPI-spectrum recorded at 270 nm. At this wavelength polycyclic aromatic molecules can be resonantly ionized and efficiently detected. In contrast, phenyl itself as well as smaller molecules

Published on 05 October 2015. Downloaded by Radboud Universiteit Nijmegen on 01/02/2016 10:52:33.

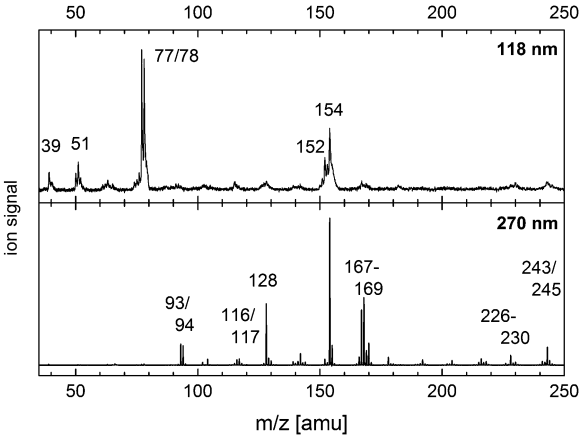

Fig. 1 Photoionisation mass spectra recorded at 118 nm (upper trace) and 270 nm (lower trace).

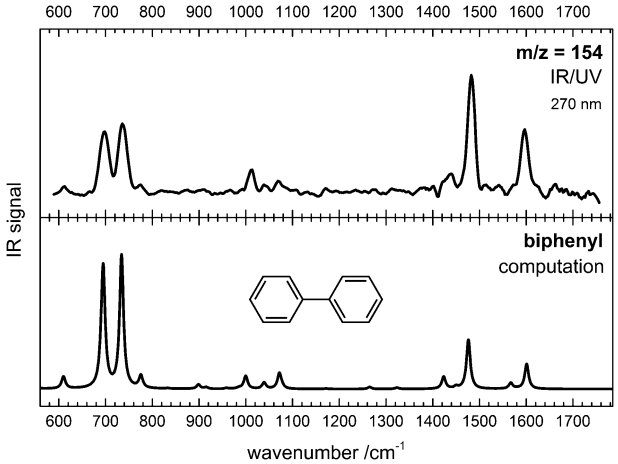

Fig. 2 The IR spectrum of the m/z = 154 reaction product (upper trace) is assigned to biphenyl based on a comparison with the computed spectrum (lower trace).

that originate from the decomposition of phenyl, *i.e.* propargyl at m/z = 39, C_4H_x and C_5H_x species are hardly visible at 270 nm. Note that propargyl was supposedly not observed in previous experiments using pure nitrosobenzene,[21] but is visible in the 118 nm photoionisation mass spectrum. The condensation products are present in both spectra, although the intensities are different due to the resonant enhancement at 270 nm. A particularly interesting peak appears at m/z = 93. Based on a REMPI scan without pyrolysis it was identified as being due to aniline (see Fig. S1 in the ESI†). This compound is present as an impurity in the commercial azobenzene sample. Note that it was not be detected by NMR spectroscopy, so its concentration has to be smaller than 1%.

Phenyl chemistry: IR-spectra of the reaction products

In the following section we will discuss the IR/UV-spectra of the reaction products observed in the mass spectrum. From the IR spectrum of the weak m/z = 77 peak it is concluded that it originates from dissociative photoionisation of m/z = 154. No spectrum was recorded for phenyl radical itself, because it could not be ionized resonantly at the excitation wavelengths employed in the experiments. The extinction coefficients ε were determined in Ar matrix.[33] The long lived A $^2B_1$ state with the origin at 510.5 nm has only a small extinction coefficient of ε = 2.8 l (mol cm)$^{-1}$. The B $^2A_1$ state has ε = 220 l (mol cm)$^{-1}$ at 235.1 nm, whereas the most intense transition to the $^2B_2$ state maximizes at 211.5 nm, but both higher-lying states are presumably short-lived. However, we want to emphasize that most polycyclic aromatic species can be resonantly ionized between 250 and 285 nm and are thus efficiently detected. In the next sections we will discuss the IR/UV spectra of the reaction products originating from phenyl condensation. The wavelengths employed for UV excitation/resonant ionization is given in the figures. While for most species IR-spectra were obtained at all UV excitation wavelengths, for some molecules only one or two UV-wavelengths lead to the appearance of IR peaks.

Biphenyl. The simplest possible product in phenyl condensation is biphenyl at m/z = 154, which is the dominant product in both mass spectra given in Fig. 1. This shows that phenyl dimerises efficiently under our experimental conditions. Rate constants for this process have been determined by a combination of photolysis and mass spectrometry.[13] The IR-spectrum of this mass is depicted in the upper trace of Fig. 2. The comparison with the computed spectrum of biphenyl in the lower trace shows that the assignment to biphenyl is unambiguous and that no other isomer of this mass is visible. The excess energy of the reaction will be transferred in further collisions. However, dimerization of phenyl is not a simple reaction: computations indicated two possible pathways to biphenyl, one proceeding *via* a σ-recombination of the two radicals, the second one *via* a π-bond recombination, *i.e.* addition of a phenyl radical to the π-system of the other one.[14] The second channel can lead to isomers of biphenyl when triplet intermediates are involved, although the possible products were not specified by Tranter *et al.*[14] The IR spectrum shows no indication of isomers and thus demonstrates that reactions leading to m/z = 154 *via* a π-bond recombination are not important. On the other hand disproportionation (reaction I) competes efficiently with dimerization. The computations of Comandini and Brezinsky[34] revealed that the disproportionation products benzene + benzyne can also be involved in biphenyl formation. Note that the presence of both species is evident from the mass spectrum in Fig. 1. The reaction

$$C_6H_6 + C_6H_5 \rightarrow C_{12}H_{10} + H \quad \Delta_R H = -42 \text{ kJ mol}^{-1} \qquad \text{(III)}$$

thus constitutes a second possible pathway to biphenyl. Here, the excess energy is taken away by the H-atom reaction product. The reaction of benzene and triplet *ortho*-benzyne forms biphenyl even more efficiently, but since *ortho*-benzyne has a singlet ground state, we assume this reaction to be of minor relevance.

***para*-Terphenyl.** Addition of another phenyl unit to biphenyl will result in an isomer of terphenyl with m/z = 230. The reaction will be associated with loss of a hydrogen atom. Fig. 3 presents the experimental IR spectrum (top trace) for

 This journal is © the Owner Societies 2015

Published on 05 October 2015. Downloaded by Radboud Universiteit Nijmegen on 01/02/2016 10:52:33.

the peak appearing at this mass. Interestingly, the best match to the experimental spectrum is provided by *para*-terphenyl. A conventional IR spectrum of *para*-terphenyl recorded in a heated gas cell for comparison[28] is depicted in the second trace from top and matches the present spectrum in terms of both band positions and intensities. The computed spectra for the three isomers *para*- (*p*-), *meta*- (*m*-) and *ortho*- (*o*-) terphenyl are given in the lower traces of Fig. 3 and exhibit distinct differences. In particular the band at 840 cm^{-1} is red-shifted in the calculated spectra to 800 cm^{-1} and 770 cm^{-1} for *m*-terphenyl and *o*-terphenyl, respectively. Although a small contribution from the *meta*-isomer cannot be ruled out based on the very weak bands at 610 cm^{-1} and 800 cm^{-1}, its concentration is estimated to be lower than 35% (Fig. S2, ESI†). Contributions from the *ortho*-isomer are negligibly small. The condensation of phenyl radicals leads predominately to *p*-terphenyl, and thus to the same product as the dimerization of the previously investigated 1- and 3-phenylpropargyl radicals.[28] Shukla and Koshi assumed *o*-terphenyl to be the dominant product of phenyl condensation, but the assignment was based on chemical arguments rather than structural information.[12]

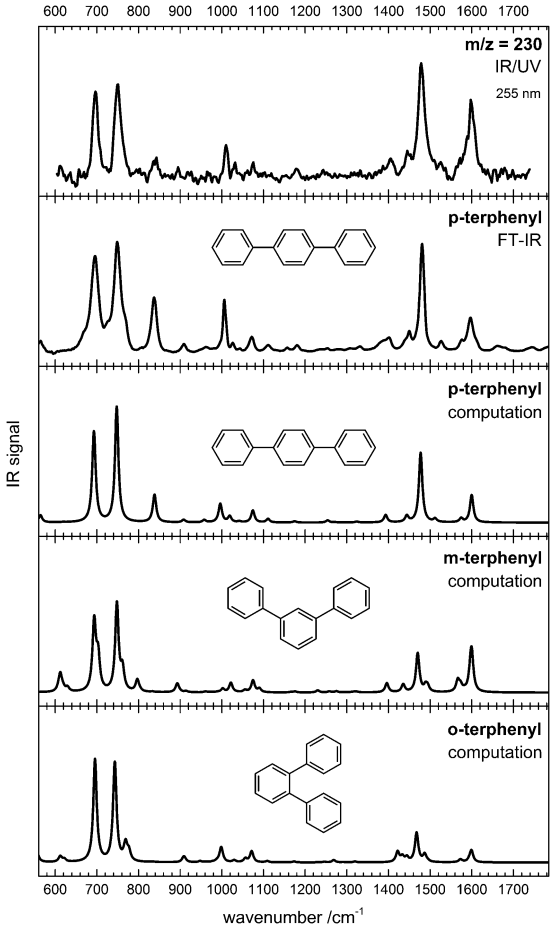

Fig. 3 The IR spectrum of the m/z = 230 reaction product (upper trace) shows that *para*-terphenyl is the preferentially formed reaction product. For comparison an experimental spectrum recorded in a heated gas cell and computed spectra of all three terphenyl isomers are given.

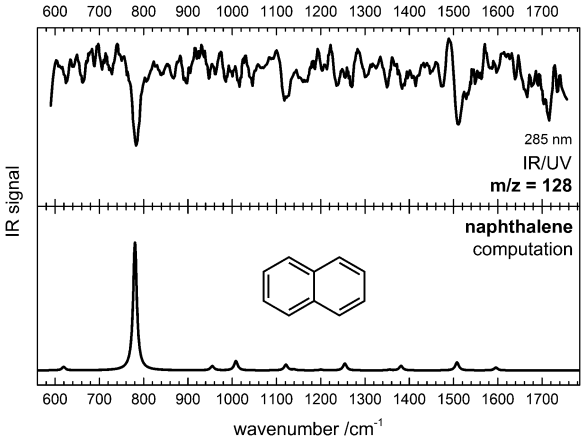

Fig. 4 Naphthalene is identified by the intense band around 790 cm^{-1} in the IR spectrum. Interestingly the IR/UV spectrum exhibits a signal gain rather than a dip.

Comandini *et al.* reported on the other hand the presence of all isomers.[11]

Naphthalene. Formation of naphthalene, $C_{10}H_8$ has already been observed in recent photoionization studies, however in the presence of acetylene.[21] It was assumed that the subsequent addition of two acetylene molecules to phenyl, followed by H-atom loss leads to the formation of this smallest PAH. In contrast, the mass spectra in Fig. 1 show a peak at m/z = 128 without addition of acetylene from the outside. The IR/UV spectra recorded at 285 nm are presented in Fig. 4. The spectrum is dominated by a single peak around 790 cm^{-1}, which is characteristic for naphthalene. Interestingly, the spectrum shows a gain in the ion signal rather than a depletion, indicating that the ionization probability is enhanced by vibrational excitation in the ground state. We conclude from Fig. 4 that naphthalene can be formed from phenyl alone without the presence of acetylene. A pathway from phenyl to naphthalene according to the reaction

$$2\ C_6H_5 \rightarrow C_{10}H_8 + C_2H_2 \quad \Delta_R H = -289\ \text{kJ mol}^{-1} \qquad \text{(IV)}$$

has been computed to proceed *via* a low activation barrier of 19 kJ mol^{-1}.[34] The transition state corresponds to a π-system addition product. The pathway includes an intersystem crossing on the way to the products. The observation of naphthalene in the phenyl system is thus supported by theory. An interesting aspect of naphthalene formation is the formation of acetylene as the second product, which can be consumed in further reactions.

1,2-Dihydronaphthalene. The IR-spectrum of the peak at m/z = 130 is shown in Fig. 5. The best match is provided by 1,2-dihydronaphthalene, given in the centre trace of the figure. The pattern with three peaks between 700 and 800 cm^{-1} is matched in both position and intensity. For comparison the computed IR-spectrum of 1,4-dihydronaphthalene is given in the lower trace of Fig. 5. It is evident that the experimental spectrum matches the one computed for the 1,2-isomer, but not the one computed for the 1,4-isomer. The observation of

Published on 05 October 2015. Downloaded by Radboud Universiteit Nijmegen on 01/02/2016 10:52:33.

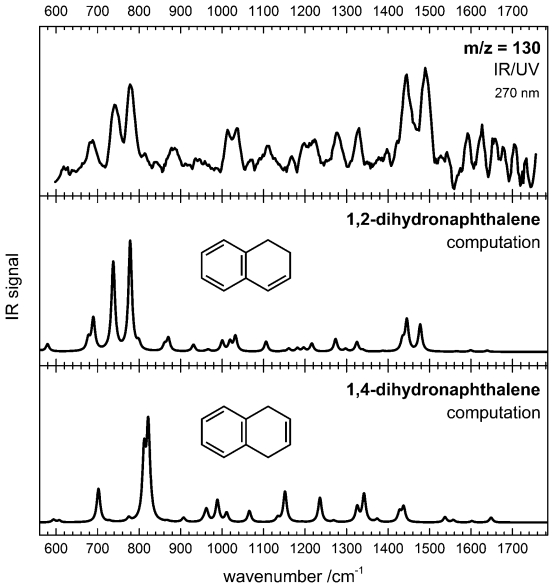

Fig. 5 The IR spectrum of the m/z = 130 reaction product (top trace) is assigned to 1,2-dihydronaphthalene on a comparison with the computed spectrum (centre trace). The spectrum of the 1,4-isomer given in the lower trace does not match.

1,2-dihydronaphthalene is not readily understood. Since hydrogenation of naphthalene is thermochemically unlikely, it has to be formed by a different route. Both crossed-beam and high-temperature pyrolysis experiments of phenyl and butadiene yielded a product at m/z = 130, which was assigned to 1,4-dihydronaphthalene based on a computed reaction pathway.[35–37] The presence of C_4H_x species from the decomposition of phenyl in the mass spectrum (upper trace of Fig. 1) indicates that this reaction can also occur in the pyrolysis reactor, but formation of 1,2-dihydronaphthalene rather than the 1,4-isomer is evident. This example shows convincingly that an isomer-selective method is required to determine the product structure and that a combination of mass spectrometry and computation is not sufficient for structure determination.

***m*/*z* = 152.** In the mass spectrum we also observed a signal at m/z = 152. Based on simple chemical arguments one would assume acenaphthene or biphenylene to be the carrier of this peak. As acenaphthene should be formed in the HACA mechanism by adding acetylene to naphthyl, its observation would provide evidence for this mechanism. In contrast, biphenylene should originate from biphenyl. Unfortunately, the signal/noise ratio of the IR-spectrum depicted in Fig. S3 of the ESI† does not permit an unambiguous identification. Two bands around 1500 cm^{-1} and 1600 cm^{-1} appear at the same position as in biphenyl and possibly originate from the dissociative photoionisation of this molecule associated with H_2-loss. In addition, the spectrum shows a characteristic peak around 1210 cm^{-1} that is not present in the spectra computed for acenaphthene or biphenylene. Furthermore a large peak computed at 722 cm^{-1} for biphenylene is not present in the experimental spectrum. Thus there is at present no evidence that either of the two compounds is formed. Other possible candidates are 1- and 2-acetylnaphthalene, but due to the low signal/noise ratio a positive identification has not yet been possible.

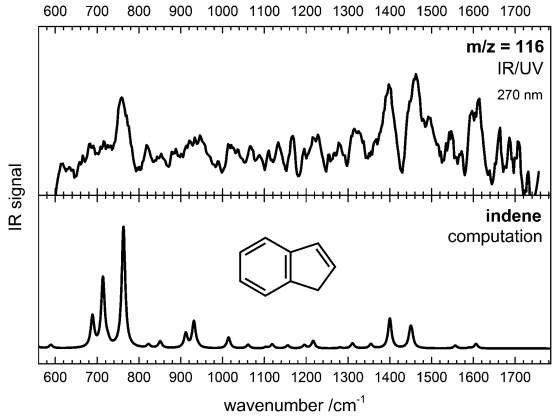

Fig. 6 The product at m/z = 116 is identified as indene.

Indene. Indene, C_9H_8 has been observed as a reaction product in a mixture of phenyl and allene or propyne.[22] Similar to naphthalene, it is detected in the present work without any secondary reactant being added. The IR/UV spectrum is given in Fig. 6, together with its computational IR spectrum. A possible mechanism can be derived from the mass spectrum recorded at 118 nm (*cf.* Fig. 1). It shows the presence of C_3H_3, which results from the decomposition of phenyl. A subsequent pathway to indene is thus

$$C_6H_5 + C_3H_3 \rightarrow C_9H_8 \quad (V)$$

It is exothermic by 944 kJ mol^{-1} and proceeds *via* a phenylpropargyl intermediate.[38] As an alternative pathway Kislov and Mebel[38] computed the reaction

$$C_6H_6 + C_3H_3 \rightarrow C_9H_8 + H \quad (VI)$$

However, (VI) is exothermic by only 62 kJ mol^{-1} and proceeds over several steps with significant activation barriers. The observation of indene here is in agreement with the one as a reaction product of phenylpropargyl.[28] The present work confirms the stability of the molecule in a high temperature environment.

Further masses. The mass spectra presented in Fig. 1 show several other masses with low intensity, which can be identified by their IR spectra. m/z = 94 corresponds to phenol (Fig. S4, ESI†), while m/z = 170 corresponds to *para*-hydroxy-biphenyl, as visible from Fig. 7 and Fig. S5 (ESI†). It seems that trace amounts of oxygen present in the pyrolysis react with the two most important species phenyl and biphenyl, forming the corresponding alcohol *via* the corresponding oxy-radical and subsequent hydrogen abstraction. This reaction has also been observed before.[21] A peak at m/z = 66 shows an IR spectrum identical to the one of phenol (Fig. S4, ESI†) and is thus assigned to a dissociative photoionisation fragment. The formation of cyclopentadiene by H-atom addition to cyclopentadienyl as suggested in ref. 21 is thus considered to be unlikely. A small peak at m/z = 104 is assigned to styrene, Ph–CH=CH_2, which indicates that a reaction with C_2 units might take place in the reactor (Fig. S6, ESI†). Note that the formation of naphthalene is

 This journal is © the Owner Societies 2015

Published on 05 October 2015. Downloaded by Radboud Universiteit Nijmegen on 01/02/2016 10:52:33.

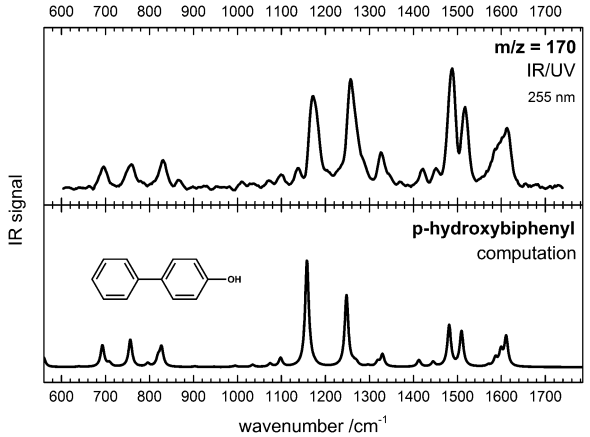

Fig. 7 The IR spectrum of m/z = 170 (upper trace) can be explained by the reaction with traces of oxygen, which leads to the formation of *para*-hydroxy-biphenyl.

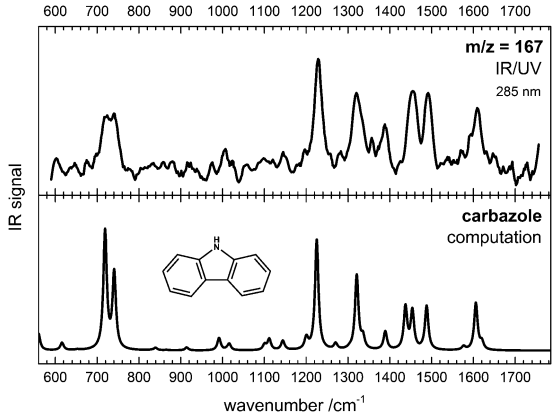

Fig. 8 Based on the computations (lower trace) the IR spectrum of the m/z = 167 reaction product (upper trace) is assigned to carbazole.

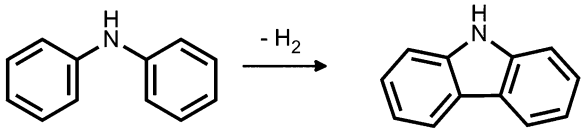

Scheme 1 Carbazole is likely formed from diphenylamine.

associated with the formation of acetylene, which can form styrene in a further reaction with phenyl. A further group of peaks appears at m/z = 140–144. m/z = 142 is identified as 1-methylnaphthalene. Its ^{13}C isotopologue also contributes to the signal at m/z = 143. In contrast, the small peaks at m/z = 140 and 144 could not be identified. Finally another small peak is found at m/z = 228. This mass was present with significant intensity in our previous work on the phenylpropargyl radicals.[28] It was a major surprise of this work when the IR spectrum was assigned to 1-(phenylethynyl)naphthalene (1-PEN), see Fig. 5 in ref. 28 and Fig. 1 in ref. 39. In the phenyl experiments, the signal in this mass channel was small and the IR spectrum rather noisy. However, 1-PEN can be ruled out as the carrier of this mass. The IR spectrum (Fig. S7, ESI†) is dominated by a single peak at 730 cm^{-1}, all further peaks are small. We therefore assign m/z = 228 to triphenylene, which has an IR-spectrum with only few bands due to its high symmetry.

Phenyl plus aniline chemistry: IR-spectra of the reaction products

The mass spectrum recorded at 270 nm shows a few smaller peaks at m/z = 117, m/z = 167–169 and 243–245, which cannot be explained by phenyl condensation.

The largest of these peaks is the one at m/z = 167. Based on the spectrum in Fig. 8 and a comparison with the computation in the lower trace it is convincingly assigned to carbazole. The IR/UV spectra at the other masses demonstrate indole (m/z = 117, Fig. S8), diphenylamine (m/z = 169, Fig. S9), phenylcarbazole (m/z = 243, Fig. S10) and triphenylamine (m/z = 245, Fig. S11) to be the carriers, which are unambiguously identified by the IR spectra given in the ESI.† They appear only with small concentration in the mass spectra. The comparably high quality of the IR spectra is most likely due to an enhancement of the absorption cross section by the dipolar NR_2–H group.

The observation of compounds containing nitrogen is at first glance surprising. Pyrolysis of azobenzene yields phenyl and N_2, the latter being unreactive. The formation of N-containing compounds might be explained by a side reaction in the pyrolysis leading to two phenylnitrene molecules. However, the presence of trace amounts of aniline, identified in a REMPI-scan without pyrolysis provides an alternative explanation for these compounds. Reactions of aniline with phenyl will lead to diphenyl- and triphenylamine. Carbazole will then be formed from diphenylamine by loss of H_2 (Scheme 1).

The efficient growth of larger rings from a reaction of phenyl and aniline has consequences for combustion of biofuel, which often contains organically bound nitrogen.[40] Here, the mechanism based on condensation of aromatic species might be very efficient and lead quickly to large ring systems containing nitrogen molecules.

Discussion

First of all, the data presented above confirm that bimolecular reactions at high temperature can be investigated in a pyrolysis microreactor. The chemistry is similar to the one proceeding in more complex setups, like shock tubes[14] or in a 56 cm quartz reactor.[12] We emphasize that the degree of secondary reactions in the reactor can be controlled by several parameters, such as the precursor concentration, lengths of the SiC tube, pyrolysis temperature, and backing gas pressure. While in a continuous expansion at low pressure significant dimerization takes place,[20,24] it can in principle be suppressed in a pulsed jet. However, in the present experiments we deliberately maintained conditions that favour bimolecular reactions and observed them by choosing a suitable delay between laser and pulsed valve.

It was found in computations that only a part of PAH formation can be explained by the HACA mechanism.[1,10] Subsequently, it was suggested that a mechanism based on the

Published on 05 October 2015. Downloaded by Radboud Universiteit Nijmegen on 01/02/2016 10:52:33.

addition of phenyl units can rationalise the rapid formation of PAHs in a few steps.[12] Here, we confirm the relevance of this mechanism and identify important reaction products by their IR spectra. The simplest reaction product, biphenyl is expected to appear with significant intensity in the presence of phenyl. The absence of other product isomers shows the selectivity of this process.

A comparison to the work by Tranter *et al.*[14] and by Shukla and Koshi is instructive,[12] who previously studied reactions of phenyl in much larger reactors. Both the EI mass spectrum[14] and the photoionization mass spectra[12] recorded at 1100 to 1200 K are very similar to the one presented above. This shows that the properties of the SiC microreactor resemble those of the much larger reactors employed so far for studying high temperature reactions. Many of the assignments of the work by Shukla and Koshi are confirmed.[12] One notable difference concerns the peak at m/z = 230. Shukla and Koshi detected a peak at m/z = 230, but assumed *o*-terphenyl to be the dominant product. The IR-spectrum in Fig. 3 shows that the *para*-isomer of terphenyl dominates, with some *meta*-isomer being possibly present. The contribution of *o*-terphenyl is negligibly small. Most likely the *ortho*-isomer cyclises according to

$$o\text{-terphenyl} \rightarrow \text{triphenylene} + H_2 \qquad \text{(VII)}$$

as suggested,[12] while the *para*-isomer remains in the reaction mixture. This observation has impact on the mechanism of further growth. Addition of a further phenyl unit to *p*-terphenyl will open additional routes to larger PAHs that have not yet been considered. Another difference concern the assignment of the m/z = 152 peak to biphenylene. We find some contribution from dissociative photoionisation of biphenyl to this peak, but the major peak in the IR spectrum is not in agreement with computations for biphenylene. Thus the identity of the m/z = 152 product is not yet clear. Note that Shukla and Koshi used benzene as a phenyl precursor, so one product of the phenyl self-reaction was present as a reactant. This potentially obscures some of the possible reaction channels.

We also want to compare our data with the work by Parker *et al.*, who conducted an experiment on a phenyl/acetylene mixture in a microreactor similar to ours.[21] Interestingly, Parker *et al.* observed no tricyclic molecules at all, which indicates that the HACA mechanism is much less efficient than phenyl addition under the appropriate pyrolysis reactor conditions. Furthermore neither C_3H_3 nor C_5H_5 were supposedly observed without acetylene being present, whereas the PIMS in the upper trace of Fig. 1 shows the presence of C_3H_3. C_5H_5 on the other hand originates from dissociative photoionisation of phenol (see above). The formation of naphthalene constitutes a further interesting aspect. Within the HACA mechanism, naphthalene is formed from phenyl by sequential addition of two acetylene units. Parker *et al.* observed naphthalene and took this as evidence for the HACA mechanism. The work presented here shows that naphthalene can be formed from phenyl alone as suggested by computational work[34] and does not require acetylene as an additional reactant. Observation of naphthalene should thus not serve as evidence for the HACA mechanism. Nevertheless, an interesting aspect of (IV) is the formation of acetylene as a side product, which can in principle participate in further processes, for example the formation of styrene, which was also identified by its IR-spectrum. By necessity the amount of naphthalene formed by the HACA mechanism from the acetylene side product has to be significantly smaller than the amount produced *via* (IV). Another possible source of acetylene in the present experiment is decomposition of benzene to C_4 and C_2 hydrocarbons.

The propensity for *p*-terphenyl has been observed before in our study on phenylpropargyl dimerization.[28] There we argued that *p*-terphenyl is favoured kinetically, because it can be readily formed in the dimerization of both 1- and 3-phenyl-propargyl. The pronounced propensity for *p*-terphenyl formation in the present work indicates the central role of this species in PAH-formation, which to the best of our knowledge has not yet been properly addressed by theory. The second product of the phenylpropargyl dimerization, 1-PEN was not identified in the present work. Since a small amount of propargyl from the pyrolysis of phenyl is detected in the mass spectrum, a formation of C_9-species is likely. Fig. 6 indicates that indene is the dominant product. It is probably formed directly by the phenyl + propargyl reaction given in (V).

Conclusions

In this work we analysed the products of the phenyl radical self-reaction by IR/UV double resonance spectroscopy. The results demonstrate that a pyrolysis microreactor mimics larger reactors used so far to study high temperature reactions. Thus the investigation of combustion relevant reactions can be conducted with such a microreactor and be combined with new laser-based detection techniques. When the growth of larger units, *i.e.* PAH or soot is studied, an isomer selective detection technique is necessary. Within this work we show that an analysis that is based on simple photoionisation mass spectrometry and chemical intuition cannot always predict chemical structures correctly. Even when photoionisation is combined with a tunable light source correct assignment is difficult, because ionization energies for different isomers are often close. In the present work we base the analysis on IR/UV double resonance spectroscopy. The method combines the mass sensitivity of resonant photoionisation ([1+1] REMPI) with the isomer sensitivity of infrared spectroscopy and is well suited for multiplex-detection of reaction products in a mixture. In addition, resonant excitation is very sensitive and allows the detection of products that are present only in small contributions and cannot be identified by simple photoionisation mass spectrometry.

The work shows that phenyl addition is a pathway that leads to rapid growth and the formation of PAHs with three aromatic rings within the microreactor. *para*-Terphenyl was identified to be the carrier of the mass signal at m/z = 230, a result that will be important for the modelling of growth to larger PAHs. Furthermore, the experiments demonstrate that species like naphthalene are formed without the addition of acetylene, as predicted by theory. Observation of naphthalene does therefore not constitute evidence for the HACA mechanism.

 This journal is © the Owner Societies 2015

Published on 05 October 2015. Downloaded by Radboud Universiteit Nijmegen on 01/02/2016 10:52:33.

The presence of small (<1%) amounts of aniline lead to the observation of various PAHs containing N-atoms. The results have a bearing on the formation of PAHs and soot in biofuels, because phenyl addition to amines is assumed to be rapid and efficient.

Acknowledgements

This work was supported by the German Science Foundation, DFG through contract FI 575/8-2. HCS acknowledges a fellowship by the 'Fonds der Chemischen Industrie'. We gratefully acknowledge the Stichting voor Fundamenteel Onderzoek der Materie (FOM) for the support of the FELIX Laboratory. The research leading to these results has received funding from the European Community's Seventh Framework Programme (FP7/2007-2013) under grant agreement no. 312284.

References

1 H. Richter, T. G. Benish, O. A. Mazyar, W. H. Green and J. B. Howard, *Proc. Combust. Inst.*, 2000, **28**, 2609.
2 A. M. Mastral and M. S. Callen, *Environ. Sci. Technol.*, 2000, **34**, 3015.
3 C. H. Wu and R. D. Kern, *J. Phys. Chem.*, 1987, **91**, 6291.
4 N. M. Marinov, M. J. Castaldi, C. F. Melius and W. Tsang, *Combust. Sci. Technol.*, 1997, **128**, 295.
5 U. Alkemade and K.-H. Homann, *Z. Phys. Chem.*, 1989, **161**, 19.
6 J. A. Cole, J. D. Bittner, J. P. Longwell and J. B. Howard, *Combust. Flame*, 1984, **56**, 51.
7 M. Frenklach, *Phys. Chem. Chem. Phys.*, 2002, **4**, 2028.
8 H. Wang and M. Frenklach, *J. Phys. Chem.*, 1994, **98**, 11465.
9 M. Frenklach, D. Clary, W. C. J. Gardiner and S. E. Stein, *Proc. Combust. Inst.*, 1985, **20**, 887.
10 V. V. Kislov, A. I. Sadovnikov and A. M. Mebel, *J. Phys. Chem. A*, 2013, **117**, 4794–4816.
11 A. Comandini, T. Malewicki and K. Brezinsky, *J. Phys. Chem. A*, 2012, **116**, 2409.
12 B. Shukla and M. Koshi, *Phys. Chem. Chem. Phys.*, 2010, **12**, 2427.
13 J. Park and M. C. Lin, *J. Phys. Chem. A*, 1997, **101**, 14.
14 R. S. Tranter, S. J. Klippenstein, L. B. Harding, B. R. Giri, X. Yang and J. H. Kiefer, *J. Phys. Chem. A*, 2010, **114**, 8240.
15 D. W. Kohn, H. Clauberg and P. Chen, *Rev. Sci. Instrum.*, 1992, **63**, 4003.
16 Q. Guan, K. N. Urness, T. K. Ormond, D. E. David, G. B. Ellison and J. W. Daily, *Int. Rev. Phys. Chem.*, 2014, **33**, 447.
17 A. Vasiliou, M. R. Nimlos, J. W. Daily and G. B. Ellison, *J. Phys. Chem. A*, 2009, **113**, 8540.
18 M. Scheer, C. Mukarakate, D. J. Robichaud, G. B. Ellison and M. R. Nimlos, *J. Phys. Chem. A*, 2010, **114**, 9043.
19 G. T. Buckingham, T. K. Ormond, J. P. Porterfield, P. Hemberger, O. Kostko, M. Ahmed, D. J. Robichaud, M. R. Nimlos, J. W. Daily and G. B. Ellison, *J. Chem. Phys.*, 2015, **142**, 044307.
20 T. Schüßler, H.-J. Deyerl, S. Dümmler, I. Fischer, C. Alcaraz and M. Elhanine, *J. Chem. Phys.*, 2003, **118**, 9077.
21 D. S. N. Parker, R. I. Kaiser, T. P. Troy and M. Ahmed, *Angew. Chem., Int. Ed.*, 2014, **53**, 7740.
22 F. Zhang, R. I. Kaiser, V. V. Kislov, A. M. Mebel, A. Golan and M. Ahmed, *J. Phys. Chem. Lett.*, 2011, **2**, 1731.
23 D. S. N. Parker, R. I. Kaiser, B. Bandyopadhyay, O. Kostko, T. P. Troy and M. Ahmed, *Angew. Chem., Int. Ed.*, 2015, **54**, 5421.
24 M. Lang, F. Holzmeier, I. Fischer and P. Hemberger, *J. Phys. Chem. A*, 2013, **117**, 5260–5268.
25 P. Oßwald, P. Hemberger, T. Bierkandt, E. Akyildiz, M. Köhler, A. Bodi, T. Gerber and T. Kasper, *Rev. Sci. Instrum.*, 2014, **85**, 025101.
26 J. Bouwman, A. Bodi, J. Oomens and P. Hemberger, *Phys. Chem. Chem. Phys.*, 2015, **17**, 20508.
27 K. H. Fischer, P. Hemberger, I. Fischer and A. M. Rijs, *ChemPhysChem*, 2010, **11**, 3228.
28 K. H. Fischer, J. Herterich, I. Fischer, S. Jaeqx and A. M. Rijs, *J. Phys. Chem. A*, 2012, **116**, 8515.
29 D. Oepts, A. F. G. van der Meer and P. W. van Amersfoort, *Infrared Phys. Technol.*, 1995, **36**, 297.
30 G. von Helden, D. van Heijnsbergen and G. Meijer, *J. Phys. Chem. A*, 2003, **107**, 1671.
31 A. M. Rijs and J. Oomens, *Top. Curr. Chem.*, 2015, **364**, 1.
32 M. J. Frisch, G. W. Trucks, H. B. Schlegel, G. E. Scuseria, M. A. Robb, J. R. Cheeseman, G. Scalmani, V. Barone, B. Mennucci, G. A. Petersson, H. Nakatsuji, M. Caricato, X. Li, H. P. Hratchian, A. F. Izmaylov, J. Bloino, G. Zheng, J. L. Sonnenberg, M. Hada, M. Ehara, K. Toyota, R. Fukuda, J. Hasegawa, M. Ishida, T. Nakajima, Y. Honda, O. Kitao, H. Nakai, T. Vreven, J. A. Montgomery Jr., J. E. Peralta, F. Ogliaro, M. Bearpark, J. J. Heyd, E. Brothers, K. N. Kudin, V. N. Staroverov, R. Kobayashi, J. Normand, K. Raghavachari, A. Rendell, J. C. Burant, S. S. Iyengar, J. Tomasi, M. Cossi, N. Rega, J. M. Millam, M. Klene, J. E. Knox, J. B. Cross, V. Bakken, C. Adamo, J. Jaramillo, R. Gomperts, R. E. Stratmann, O. Yazyev, A. J. Austin, R. Cammi, C. Pomelli, J. W. Ochterski, R. L. Martin, K. Morokuma, V. G. Zakrzewski, G. A. Voth, P. Salvador, J. J. Dannenberg, S. Dapprich, A. D. Daniels, O. Farkas, J. B. Foresman, J. V. Ortiz, J. Cioslowski and D. J. Fox, *Gaussian 09*, *Revision B.01 edn*, Gaussian Inc., Wallingford CT, 2009.
33 J. G. Radziszewski, *Chem. Phys. Lett.*, 1999, **301**, 565.
34 A. Comandini and K. Brezinsky, *J. Phys. Chem. A*, 2011, **115**, 5547.
35 R. I. Kaiser, D. S. N. Parker and A. M. Mebel, *Annu. Rev. Phys. Chem.*, 2015, **66**, 43.
36 R. I. Kaiser, D. S. N. Parker, F. Zhang, A. Landera, V. V. Kislov and A. M. Mebel, *J. Phys. Chem. A*, 2012, **116**, 4248.
37 A. Golan, M. Ahmed, A. M. Mebel and R. I. Kaiser, *Phys. Chem. Chem. Phys.*, 2013, **15**, 341.
38 V. V. Kislov and A. M. Mebel, *J. Phys. Chem. A*, 2007, **111**, 3922.
39 P. Constantinidis, M. Lang, J. Herterich, I. Fischer, J. Auerswald and A. Krueger, *J. Phys. Chem. A*, 2014, **118**, 2915.
40 K. Kohse-Höinghaus, P. Oßwald, T. A. Cool, T. Kasper, N. Hansen, F. Qi, C. K. Westbrook and P. R. Westmoreland, *Angew. Chem., Int. Ed.*, 2010, **49**, 3572.